Approximate stacking velocities in a weakly transversely anisotropic layer

Björn E. Rommel

ABSTRACT

For weak anisotropy as defined by Thomsen and according to his scheme, approximations of the moveout velocity and traveltime of *PP* and *SVSV* waves reflected at the bottom of a single layer are presented in the form of an offset-dependent polynomial. The moveout velocity does not only differ from the vertical ray velocity as already pointed out by Thomsen, but varies with offset depending on the anisotropy coefficients. This variation gives rise to non-hyperbolic traveltime curves. If this effect is not taken into account, stacking will likely deteriorate. The variation is most pronounced in the *SVSV*-case, especially if the medium is characterized by a negative value of the difference of two of Thomsen's anisotropy coefficients, $(\varepsilon - \delta)$. This behaviour also explains the results of Levin's case study, since interpretation must consider the presence of anisotropy. But by using the regression method on the approximate coefficients, additional information on the *SV*-anisotropy can be obtained.

INTRODUCTION

Many crustal rocks as well as layered sequences of sediments, all relevant to seismic exploration, are found to be anisotropic. In most cases, however, the properties of these anisotropic media do not deviate much from comparable isotropic media. Therefore approximations to all the functions describing these properties are both sufficiently accurate and more easily treated than the exact ones.

The approximation scheme published by Thomsen (1986) has gained much attention. He defined so called anisotropy coefficients characterizing the deviation from isotropy. Since they are usually small in value, meaning the anisotropy is weak, all relevant equations of physical properties can be expanded into polynomials involving these coefficients. Thomsen (1986) presented first-order approximations of most physical equations relevant to seismic exploration.

However, Thomsen (1986) approximates the traveltime of a wave reflected at the bottom of a single layer only by the initial slope of the t^2 versus x^2 curve. Since even for a single anisotropic layer the squared traveltime of a reflected wave does not plot along a straight line, as it does for an isotropic layer, a constant moveout or stacking velocity is not to be expected.

In the following, Thomsen's (1986) scheme is extended to obtain an offset-dependent moveout velocity. It is an approximation of the actual slope at any offset and hence called the local moveout velocity. It is then used to obtain, by means of an integration, an approximation of the squared traveltime function of reflected *PP* and *SVSV* waves in a single layer. The squared offset-traveltime diagram has been chosen because it easily reveals any influence of anisotropy by deviations from straight lines, and since it avoids a further step in the approximation scheme.

By this means Thomsen's (1986) approximation of the *PP* and *SVSV* traveltime is improved for larger offsets. However, converted waves and multi-layer cases are not yet included.

The polynomial coefficients of the improved traveltime function depend theoretically on reflector depth, vertical velocity, and anisotropy coefficients. Numerical values can be assigned to these by means of a regression analysis. Indeed, the traveltime function presented here is an approximation of the exact traveltime, and the regression function is an approximation of the observed traveltime. But for weak anisotropy, the functions match sufficiently well.

Indeed, the possibility of this comparison between a theoretical and an observed traveltime curve is the major goal of this work. The approximation scheme has been chosen in order to obtain a linearized traveltime function, whose coefficients can numerically be determined by standard regression analysis.

By means of a Gaussian elimination process, all layer parameters governing the propagation of the *SVSV* wave can be recovered. Hence this method offers a quick means to obtain additional information on the *SV* anisotropy. Unfortunately, a Gaussian elimination process on a first-order approximation of the traveltime does not provide stable information on the *P* anisotropy.

However, the approximation of the traveltime clearly demonstrates the influence of anisotropy. Though no stacking tests have been done until now, the presence of anisotropy must obviously be taken into account in the processing and interpretation, especially in the case of *SVSV* data.

LOCAL MOVEOUT (LMO) VELOCITY

In anisotropic media the wave velocities depend on the direction of propagation. The velocity that can be observed, is the velocity of energy transport, or the ray velocity V at the ray angle ϕ. It depends on the phase velocity v at the phase angle θ, that is the velocity of the phase propagation. For a transversely isotropic medium the relationship between these velocities has already been presented by Postma (1955).

For weakly transversely anisotropic media, viz. for small anisotropy coefficients ε, δ, γ as defined by Thomsen (1986), the phase velocity $v(\theta)$ does not deviate much from the vertical velocities α_0 and β_0 of the *P* wave and the *S* waves, respectively. Thomsen (1986) proved that, to first order, the magnitude of the ray velocity V can be equated with the phase velocity v, though the ray angle ϕ corresponds to a different phase angle θ (see Figure 1a, and the left sides of the Figures 3, and 5 for extremely anisotropic cases). Then the approximate ray velocities $V(\phi)$ obtained by Thomsen (1986, eq. 20) are,

for the P wave:

$$V(\phi) \approx \alpha_0 \left(1 + \delta \sin^2 \theta \cos^2 \theta + \epsilon \sin^4 \theta\right) \tag{1a}$$

$$\text{with } \phi \approx \arctan\left\{\left[1 + 2\delta + 4(\epsilon - \delta)\sin^2\theta\right]\tan\theta\right\}, \tag{1b}$$

for the SV wave:

$$V(\phi) \approx \beta_0 \left(1 + \xi \sin^2\theta \cos^2\theta\right) \qquad \text{where}\ \xi = {\alpha_0}^2/{\beta_0}^2(\epsilon - \delta) \tag{1c}$$

$$\text{with}\ \phi \approx \arctan\left\{\left[1 + 2\xi\left(1 - 2\sin^2\theta\right)\right]\tan\theta\right\}, \tag{1d}$$

and for the SH wave:

$$V(\phi) \approx \beta_0 \left(1 + \gamma \sin^2\theta\right) \tag{1e}$$

$$\text{with}\ \phi \approx \arctan\left\{\left[1 + 2\gamma\right]\tan\theta\right\}. \tag{1f}$$

In order to compute the ray velocity and later the traveltime of a ray at a specified ray angle with Thomsen's (1986) approximation, one must reversely know the phase angle dependent on the ray angle. However, the inverse function $\theta(\phi)$ may be difficult or impossible to compute analytically. But Brown et al. (1991) showed, that for a weakly transversely anisotropic medium the first-order difference between the phase angle and the ray angle propagates into a second-order and therefore minor difference between the phase velocity and the ray velocity. To first order, the ray velocity is determined solely by the variation of the phase velocity, and the ray angle can be equated with the phase angle (see Figure 1b, and the right sides of the Figures 3, and 5 for extremely anisotropic cases).

Thomsen (1986) demonstrated the effects of an angular-dependent velocity on the traveltime with the simplest case, a reflected wave in a single layer with parallel interfaces. Even for this case the squared traveltime plots along a curved line instead of a straight line. Therefore the slope of the traveltime function varies with the angle of incidence or equivalently with the offset.

The general equation governing the slope for all offsets was already presented by Thomsen (1986, eq. 24) as:

$$\frac{\mathrm{d}\left(t^2\right)}{\mathrm{d}\left(x^2\right)} = \frac{1}{V^2(\phi)}\left[1 - \frac{2\cos^2\phi}{V(\phi)}\frac{\mathrm{d}V(\phi)}{\mathrm{d}\sin^2\phi}\right]. \tag{2}$$

Thomsen (1986) restricted his actual computation to the limit of vertical incidence. Since the direct dependence of the ray velocity on the ray angle is elaborated by Brown et al. (1991), the computation of the moveout velocity at any offset is straightforward. After inserting the approximate ray velocity (eq. 1 with θ replaced by ϕ) into the general function of the LMO velocity V_{LMO} (eq. 2) one obtains,

for the PP wave:

$${V_{\mathrm{LMO}}}^2(\phi) \approx {\alpha_0}^2\left[1 + 2\delta + 4(\epsilon - \delta)\sin^2\phi - 2(\epsilon - \delta)\sin^4\phi\right], \tag{3a}$$

and for the $SVSV$ wave:

$${V_{\mathrm{LMO}}}^2(\phi) \approx {\beta_0}^2\left[1 + 2\xi - 4\xi\sin^2\phi + 2\xi\sin^4\phi\right]. \tag{3b}$$

Since ray angles are of secondary interest the formulae can be recast in terms of offset and the desired reflector depth. For small ray angles, that is for small offsets x

compared with the reflector depth h, this relation is usually expanded in terms of offset as follows:

$$\sin^2\phi = \frac{x^2}{x^2+(2h)^2} \approx \frac{1}{(2h)^2}x^2 - \frac{1}{(2h)^4}x^4 + \frac{1}{(2h)^6}x^6 - \frac{1}{(2h)^8}x^8 \pm \ldots \tag{4}$$

The first approximation is the expansion of the LMO velocity into a polynomial in anisotropy coefficients (eq. 3) and the second is the expansion of the trigonometric function into a polynomial of offset/depth ratio (eq. 4). The two are independent of each other.

With both approximations (eq. 3, and 4) the following LMO velocity is obtained,

for the PP wave:

$$V_{\mathrm{LMO}}{}^2 \approx \alpha_0{}^2\left[1+2\delta+\frac{4(\epsilon-\delta)}{(2h)^2}x^2-\frac{6(\epsilon-\delta)}{(2h)^4}x^4+\frac{8(\epsilon-\delta)}{(2h)^6}x^6-\ldots\right], \tag{5a}$$

and for the $SVSV$ wave:

$$V_{\mathrm{LMO}}{}^2 \approx \beta_0{}^2\left[1+2\xi-\frac{4\xi}{(2h)^2}x^2+\frac{6\xi}{(2h)^4}x^4-\frac{8\xi}{(2h)^6}x^6+\ldots\right]. \tag{5b}$$

Due to the expansion of the offset/depth ratio these functions are no longer of complete first order in the anisotropy coefficients. But the additional coefficients which all are either of the form $(\varepsilon - \delta) / (2h)^{2n}$ or $\xi / (2h)^{2n}$ are small in value. According to the convergence rule of Leibniz these functions are valid for all ray angles [$\phi = \arctan(x / 2h)$] less than or equal to 45°. However, since they are usually truncated beyond the third term, one must restrict oneself to ray angles less than 39° to ensure decreasing values of the third and fourth coefficients.

The very first term, e. g. $V_{\mathrm{LMO}}{}^2 \approx \alpha_0{}^2$, would be valid for an isotropic medium with its spherical wavefronts. Together with the second term the LMO velocity of an elliptical wavefront is described. Of course only the PP wavefront can be truly elliptical ($\varepsilon = \delta \neq 0$) corresponding to a spherical $SVSV$ wavefront ($\xi = 0$). So far these LMO velocities are still constant. They are identical to those of Thomsen (1986), and simply extend his NMO velocity to any offset. For positive anisotropy coefficients (δ, and ξ) the NMO velocities are greater than the actual vertical velocities, and vice versa. But for any other offset the actual slope can deviate from the normal one by a significant amount depending on the anisotropy coefficients. Therein the sign of the difference ($\varepsilon - \delta$) determines whether the LMO velocity of the PP wave or the $SVSV$ wave increases or decreases. In any case the PP wave and the $SVSV$ wave behave oppositely, viz. an increasing PP LMO velocity and a decreasing $SVSV$ LMO velocity are mutually dependent. The LMO velocity of the $SVSV$ wave generally varies more than the LMO velocity of the PP wave since the anisotropy coefficient ξ is larger than the combination ($\varepsilon - \delta$) by the squared velocity ratio v_P^2/v_S^2 (eq. 1c).

If all restrictions, those are weak anisotropy and small ray angles are met, the subsequent terms give increasingly better approximations of the LMO velocity.

TRAVELTIME

After having obtained an approximation to the local moveout velocity (eq. 5) or reciprocal slope of the traveltime t, the traveltime itself can be computed by an integration over the offset. In this, the constant of integration is the square of the vertical traveltime t_0:

$$t^2 = {t_0}^2 + \int_0^{x^2} \mathrm{d}x'^2 \, \frac{1}{{V_{\mathrm{LMO}}}^2}. \tag{6}$$

Before integration the squared LMO velocity in the denominator is expanded as a polynomial of the anisotropy coefficients. This expansion requires only an interchange of + and - signs of all first-order terms (in eq. 5).

Then the traveltime functions read,

for the PP wave:

$$t^2 \approx \frac{(2h)^2}{{\alpha_0}^2} + \frac{1}{{\alpha_0}^2\,(1+2\delta)}x^2 - \frac{2\,(\epsilon-\delta)}{{\alpha_0}^2\,(2h)^2}x^4 + \frac{2\,(\epsilon-\delta)}{{\alpha_0}^2\,(2h)^4}x^6 - \frac{2\,(\epsilon-\delta)}{{\alpha_0}^2\,(2h)^6}x^8 \pm .. \tag{7a}$$

and for the $SVSV$ wave:

$$t^2 \approx \frac{(2h)^2}{{\beta_0}^2} + \frac{1}{{\beta_0}^2\,(1+2\xi)}x^2 + \frac{2\xi}{{\beta_0}^2\,(2h)^2}x^4 - \frac{2\xi}{{\beta_0}^2\,(2h)^4}x^6 + \frac{2\xi}{{\beta_0}^2\,(2h)^6}x^8 \mp .. \tag{7b}$$

The first term gives the well known vertical traveltime. The second term describes the increase of traveltime with offset for an elliptic wavefront. Here the anisotropy coefficients have been moved into the denominator. Though there should be no difference in a first-order approximation, this form provides a better match with the exact traveltime. Then the next terms describe deviations from the elliptic wavefront. With increasing offset these deviations become more and more important (see Figure 2).

As described above, the offset dependency of the *PP* and *SVSV* waves behave oppositely. If e. g. the traveltime of the *PP* wave increases more than one would expect based on the NMO velocity, the traveltime of the *SVSV* wave increases less than expected. In any case the deviation from the linear increase in traveltime with offset is larger (scaled by the squared velocity ratio) for the *SVSV* wave than for the *PP* wave.

On the whole, the traveltime approximation tries to match the traveltime of the approximate rather than the exact wavefront (see the right sides of the Figures 3, and 5 for extremely anisotropic cases). The deviation between the exact and the approximate phasefront, which replaces the wavefront in the first-order approximation (see section on the LMO-velocity), is one, but not the main cause of a mismatch. The deviation between the ray and the phase angle is, though of higher order (see the same section), not to be overlooked.

Generally Thomsen's (1986) approximation of the NMO velocities as well as the scheme presented here work better with large positive values rather than with large negative values of the anisotropy coefficient. This behaviour is caused by the nonlinear dependency of the ray angle on the phase angle, as can be seen by the complete linearization of Thomsen's (1986, eq. 22) approximation in terms of anisotropy coefficients;

for the P wave:

$$\phi \approx \theta + 2\delta \sin\theta \cos\theta + 4(\epsilon - \delta)\sin^3\theta \cos\theta, \tag{8a}$$

for the SV wave:

$$\phi \approx \theta + 2\xi \sin\theta \cos\theta - 4\xi \sin^3\theta \cos\theta, \tag{8b}$$

and for the SH wave:

$$\phi \approx \theta + 2\gamma \sin\theta \cos\theta. \tag{8c}$$

With a positive value the ray angle increases with respect to the phase angle for near-vertical incidence, but with a negative value the ray angle decreases. If one looks at a fixed offset, and therefore at a fixed range of ray angles, a smaller interval of phase angles is covered with a positive value and vice versa. With the same absolute value of the coefficients the variation of ray velocities found within the fixed offset is smaller for positive values rather than with negative values. Therefore the near-vertical curvature changes less, and the exact wavefront matches a suitable ellipse better. Consequently the traveltime curve looks smoother, allowing a better regression and an easier approximation. Since the approximation presented here does not take into account the deviation of the ray angle from the phase angle, its validity is restricted to a relatively smaller offset or to smaller absolute values for media being characterized by negative values rather than by positive values of the anisotropy coefficients. In addition, due to more terms depending on the offset, the improved approximation is less robust than Thomsen's (1986) if the restriction of weak anisotropy is nearly violated.

Nevertheless, under these preconditions the improved approximation clearly demonstrates the influence of anisotropy on the traveltime. Especially the *SVSV* wave reacts sensitively to the presence of anisotropy. Depending on the sign and magnitude of the anisotropy coefficient ξ, the traveltime curve can be strongly convex. Though no stacking tests have been done until now, stacking is likely deteriorated if anisotropy and, hence, the deviation of the squared traveltime from a straight (regression) line is not taken into account.

INFORMATION CONTENT

The traveltime (eq. 7) is the theoretical approximation of the exact traveltime with known layer parameters. In seismic processing, obtaining optimum parameters is the goal. The observed squared traveltime is approximated by a regression function of the form $t^2 = k_0 = k_2 x^2 + k_4 x^4 + \ldots$. Each coefficient sets up an independent equation between the numerical value on the one side and depth, velocity and anisotropy coefficients on the other side. The propagation of the *SVSV* wave is governed by three parameter: depth, velocity and the parameter ξ. With a direct Gaussian elimination procedure these layer parameters are recovered, as follows:

$$\xi \approx \frac{k_0 k_4}{2{k_2}^2}, \tag{9a}$$

$$ {\beta_0}^2 = \frac{1+2\xi}{k_2}, \tag{9b}$$

$$(2h)^2 = k_0 {\beta_0}^2. \tag{9c}$$

The propagation of the *PP* wave is different from that of the *SVSV* wave as it is governed by four unknowns: depth, velocity, the coefficient δ and the combination ε - δ. But if the restriction to first-order approximation is applied throughout the elimination process, sixth- and higher-order terms are always solved for the same anisotropy coefficients ε - δ for the *PP* wave (resp. ξ for the *SVSV* wave). Therefore they do not give any additional information. Since only the first three coefficients can be used, the layer parameters governing the *PP* wave cannot be recovered in a similiar way. Anyway, to obtain stable information an anisotropy its influence must be clearly observable. Here, the observable effect is the deviation of the traveltime curve from a straight line. For the *PP* wave in most media the deviation is probably too small. This gives rise to good stacking results, but provides only the moveout velocity rather than the true ray velocity.

Surprisingly, the most sensitive wave, namely the *SVSV* wave, gives access to the easiest interpretation. Several numerical tests show that the interpretation suggested above does improve the estimation of velocity and reflector depth compared with a simple analysis of a straight regression line. But the quality of the interpretation deteriorates with a larger, especially a larger negative anisotropy coefficient.

ADDITION TO LEVIN'S CASE STUDIES

In a case study Levin (1989) investigated the traveltime of waves reflected at the bottom of a single layer. One of his goals was to compare the numerical stacking velocity as computed by regression with Thomsen's (1986) theoretical NMO velocity for the *SVSV* waves in different media. For most of these media the NMO velocities computed according to Thomsen (1986) fit the numerical stacking velocities quite well. But for some media (labelled 2, and 7) the approximation fails for the *SVSV* wave. Levin (1989) suspected the non-ellipticity of the near-vertical wavefront as the cause.

Indeed, there is a strong non-ellipticity in the exact wavefront of these cases. For example, Mesaverde mudshale, the case labelled 2, is characterized by a large negative anisotropy coefficient ξ of -0.497 (see Figure 3). Such a value is very close to -0.5, below which at least Thomsen's (1986) approximation of the ray angle indicates a loop in the wavefront. The transition from non-cuspoidal into cuspoidal behaviour is smooth, viz. the exact wavefront of Mesaverde mudshale is already effected by the vicinity to cuspoidal behaviour. Therefore the near-vertical ray velocity decreases rapidly. This decrease corresponds to a rapidly increasing traveltime (see Figure 4). Hence the NMO velocity is extremely small. Nevertheless the approximate NMO velocity of 211 *m/s* does perfectly fit the numerical NMO velocity computed by regression over an extremely short spread. But the decrease of the ray velocity goes down, meaning a rapid change of the near-vertical curvature and a strongly convex traveltime curve. Therefore the LMO velocity increases rapidly limiting the match with the approximate NMO velocity to extremely small 0.01°. Unfortunately a first-order approximation to the LMO velocity and, hence, the traveltime is not appropriate to describe such an extreme behaviour, and does not improve Thomsen's (1986) approximation. For this purpose the value of the anisotropy coefficient is far beyond the restriction of weak anisotropy. But interpreting a traditional straight regression line would result in severe errors of velocity and depth, assumed that stacking along that line would work at all.

On the other hand, Dog Creek shale is an example of rock with a large positive anisotropy coefficient ξ=0.643 (see Figure 5). Though the absolute value is even larger, the approximate NMO velocity matches the numerical stacking velocity rather well (Levin, 1989; see Figure 6). That is why the ray velocity does not change much in the corresponding small interval of phase angles (see eq. 8b). Though the approximated wavefront grossly overestimates the exact wavefront, restricted to near-vertical offsets the approximate ray velocity is still sufficient. Unfortunately, the improved approximation of the traveltime is more sensitive to anisotropy than Thomsen's (1986) original one as it does not allow such a large positive anisotropy coefficient. However, in contrast to Mesaverde mudshale, an interpretation of a straight regression line would indeed work here, but would also result in severe errors of velocity and depth, since the stacking velocity disagrees with the exact vertical velocity.

The two media, Mesaverde mudshale and Dog Creek shale, represent different properties of *SV* wave propagation. They have been chosen to explain the contradictory results of Levin's (1989) case study. However, they cannot be considered as weakly anisotropic. On no account should Thomsen's (1986) approximation scheme be discarded for really weakly anisotropic media.

CONCLUSIONS

Thomsen's (1986) approximation scheme and the elaboration of Brown et al. (1991) thereof allows one to develop a first-order approximation of the moveout velocity and the traveltime, here presented for the *PP* and *SVSV* waves reflected at the bottom of a single layer.

Depending on the anisotropy coefficients, the moveout velocities can vary significantly with offset. The *SVSV* wave shows a generally larger deviation of the normal moveout velocity from the exact vertical velocity and always a larger variation with offset than the *PP* wave. Therefore the *SVSV* wave proves again to be much more sensitive to anisotropy, especially if the medium is characterized by a negative value of the anisotropy coefficient ξ.

By means of an integration, an approximation to the traveltime function is obtained. The one presented here is given to first order in the anisotropy coefficients, but the expansion of the trigonometric functions is truncated. The coefficients of the polynomial are governed by depth, velocity and anisotropy coefficients.

By comparing the theoretical coefficients of the traveltime function with the numerical ones of a regression function, additional information about the layer parameters can be obtained. In particular, the layer parameters governing the propagation of the *SVSV* wave can be recovered directly by a Gaussian elimination process.

Obviously the interpretation of stacking results, especially the interpretation of *SVSV* data, can suffer significantly from inadequate consideration of anisotropy. Not only does the NMO velocity give a wrong estimation of the vertical velocity as pointed out by Thomsen (1986), but stacking itself can very likely be deteriorated if the variation of the moveout velocity is not carefully taken into account.

This effect could already be observed in Levin's (1989) case study. The NMO velocity in Mesaverde Mudshale is much more influenced than the NMO velocity in Dog Creek Shale. For Mesaverde mudshale the velocity obtained by a straight regression line would strongly depend on the spreadlength and, hence, would be of no use in interpretation. For Dog Creek shale the velocity analysis would be stable, but still differ from the vertical velocity. These effects can mainly be attributed to the signs of the anisotropy coefficient ξ and its consequences. In both cases the influence of anisotropy must not be overlooked.

ACKNOWLEDGEMENTS

My work has partially been funded by the Bundesminister für Forschung und Technologie (BMFT), Germany, and formerly Preussag, Erdöl und Erdgas, Hannover under contract no. 0326631A ANISEIS (an unintended name collision with D. Taylor's modelling software). I especially express my thanks to Prof. Dr. J. Fertig, at that time with Preussag, for this funding and not least for his encouragement and interest in the subject.

I owe Prof. Dr. A. Behle, Universität Hamburg, a great debt of gratitude for his continuous encouragement and support. And I offer my thanks to F. Ohlsen for improving my graphic programs as well as to Dr. E. Tessmer, Dr. G. Tessmer and C. Jastram for their support.

Thanks to the support of the CREWES Project, and particularly to Prof. Dr. R. J. Brown, my work is now continuing at The University of Calgary. The manuscript was carefully corrected by D. Easley and especially by Prof. Dr. R. J. Brown. Finally I acknowledge the support provided by D. Foltinek, H. Bland, and M. Lane.

REFERENCES

Brown, R. J., Lawton, D. C., Cheadle, S. P., 1991, Scaled physical modelling of anisotropic wave propagation: multioffset profiles over an orthorhombic medium: Geophys. J. Int. **107**, 693-702.

Levin, F. K., 1989, *SV* wave velocities from *P-P* and *P-SV* data for transversely isotropic solids: Geophysics **54**, 1336-1338.

Postma, G. W., 1955, Wave propagation in a stratified medium: Geophysics **20**, 780-806.

Thomsen, L., 1986, Weak elastic anisotropy: Geophysics **51**, 1954-1966.

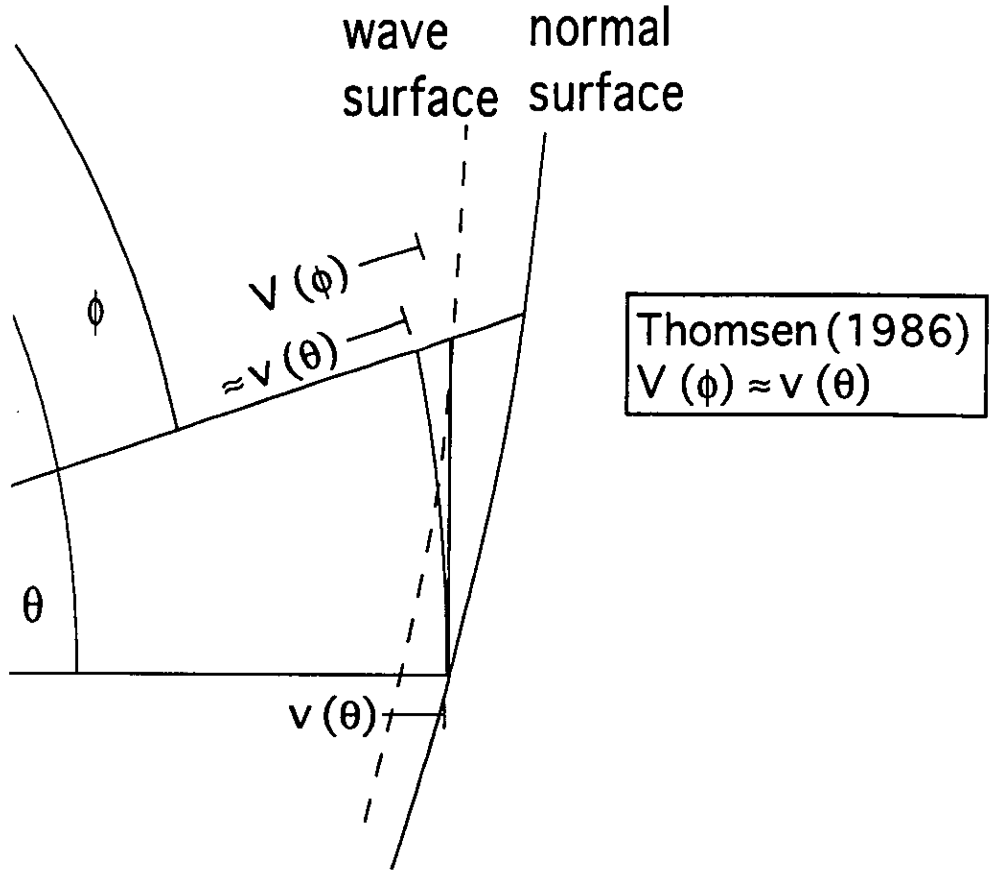

FIG. 1a: Different approximations of the exact ray velocity. Physically, a phase angle θ is assumed to correspond to a ray angle ϕ. Here, Thomsen's (1986) approximation is illustrated. The enlargement shows parts of the normal and the wave surface as well as (from the bottom to the top)

$v\ (\theta)$ the exact phase velocity $v\ (\theta)$ at the angle θ,
$\approx v\ (\theta)$ the phase velocity (of the 1st line) projected into the angle ϕ,
$V\ (\phi)$ the exact ray velocity $V\ (\phi)$ at the angle ϕ.

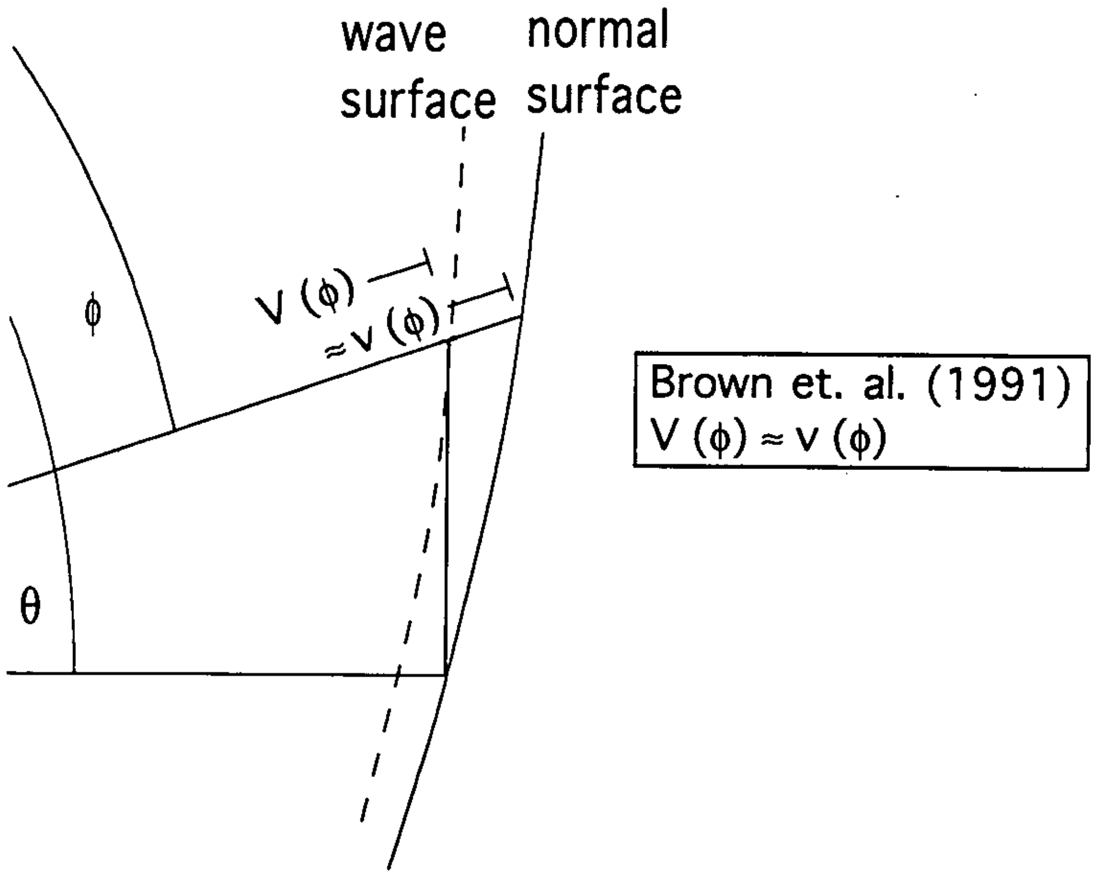

FIG. 1b: Different approximations of the exact ray velocity. Physically, a phase angle θ is assumed to correspond to a ray angle ϕ. Here, an approximation of Brown et al. (1991) is illustrated. The enlargement shows parts of the normal and the wave surface as well as (from the bottom to the top)

$v(\phi)$ the exact phase velocity $v(\phi)$ at the angle ϕ (though a phase angle θ and a ray angle ϕ do not correspond),

$V(\phi)$ the exact ray velocity $V(\phi)$ at the angle ϕ.

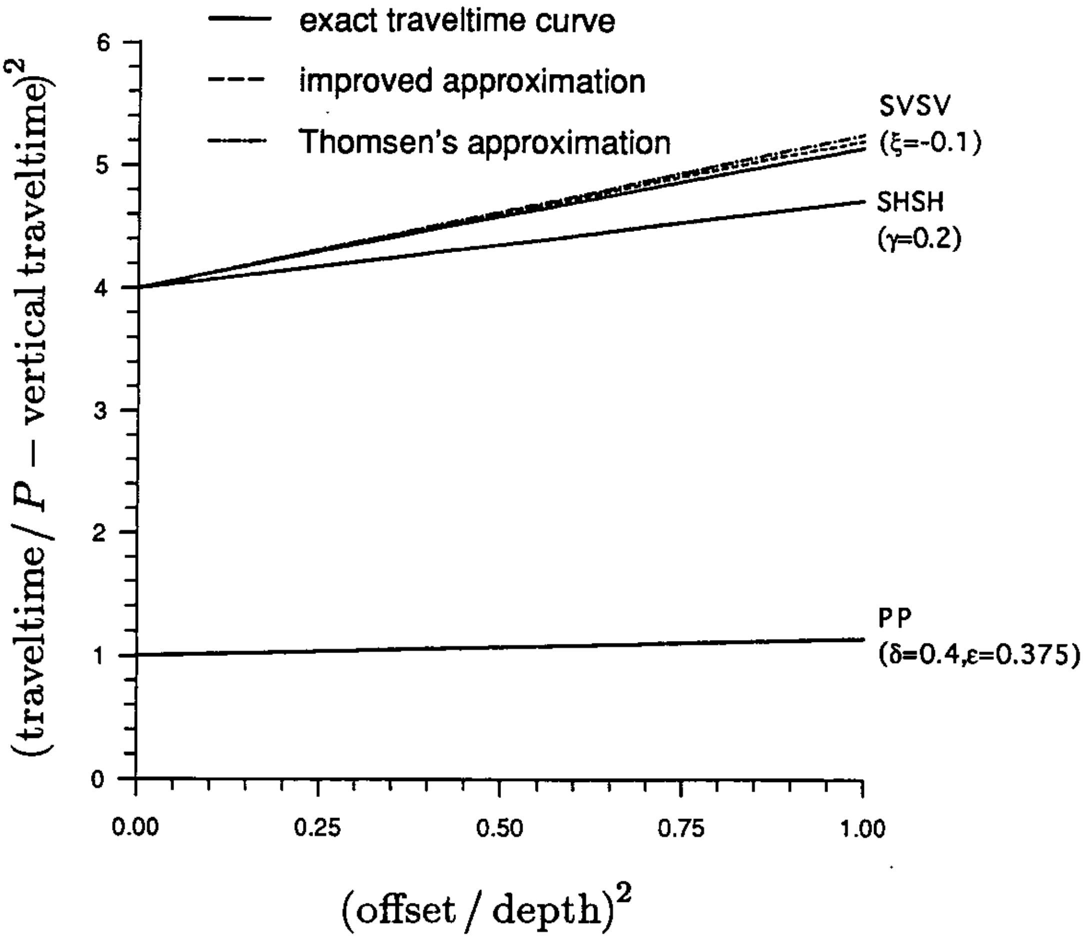

FIG. 2: Example of exact and differently approximated traveltime curves. The anisotropy coefficients have been chosen so as to yield a reasonable negative value for ξ, which governs the propagation of the *SVSV* wave. The *SHSH* traveltime curve is strictly straight, the *PP* one almost straight, so that no differences can be seen. The term *Thomsen's approximation* is used for an extension of his (1986) approximate NMO velocity to any offset. The improved approximation is truncated beyond the third term of the approximate traveltime, a series in offset/depth ratio and of first order in the anisotropy coefficients.

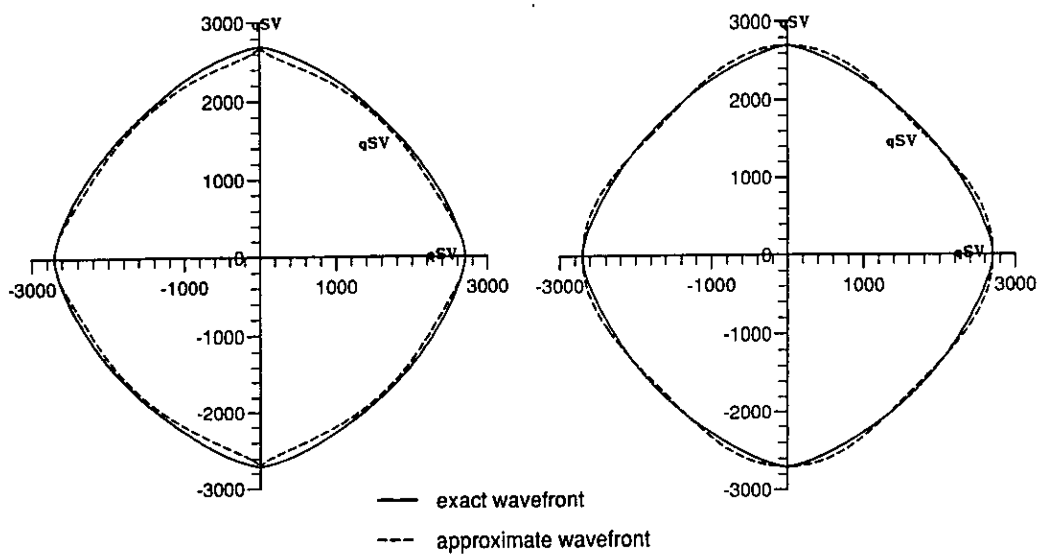

FIG. 3: Exact and approximate wave surface of Mesaverde mudshale. Notice the large near-vertical decrease of the exact ray velocity, though the extreme near-vertical change of the exact curvature can hardly be seen. The approximation is carried out

left: according to Thomsen (1986), and

right: according to Brown et al. (1991).

Here, both approximations are of the same quality.

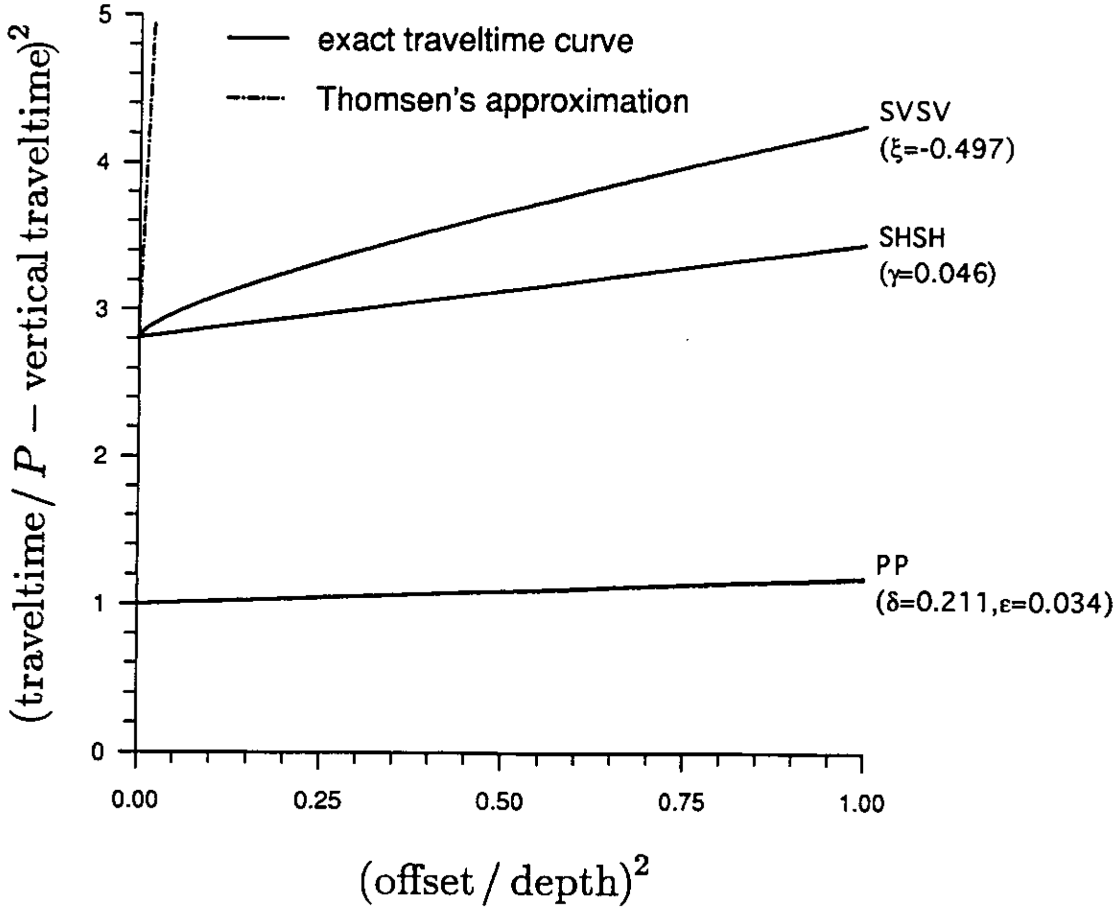

FIG. 4: Exact and approximate traveltime curves of Mesaverde mudshale. Due to the strong convexity of the *SVSV* traveltime curve indicated by a large negative anisotropy coefficient ξ, Thomsen's (1986) approximation is valid only in the immediate neighbourhood of near-vertical incidence. In contrast, the *PP* traveltime curve is hardly influenced.

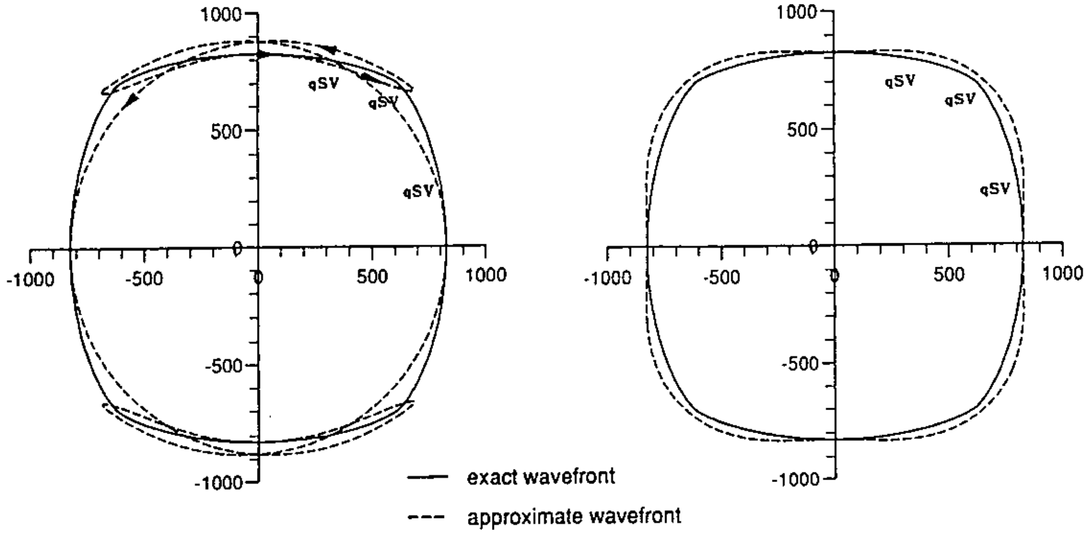

FIG. 5: Exact and approximate wave surface of Dog Creek shale. The approximation is carried out
left: according to Thomsen (1986), and
right: according to Brown et al. (1991).
The arrows in the approximate wave surface indicate the movement of the ray angle with increasing phase angle according to Thomsen's (1986) approximation, which is acceptable for near-vertical incidence and violates physics for larger angles of incidence. The approximation of Brown et al. (1991) cannot give artificial (or reproduce true) loops; but, here, it overestimates the exact wavefront.

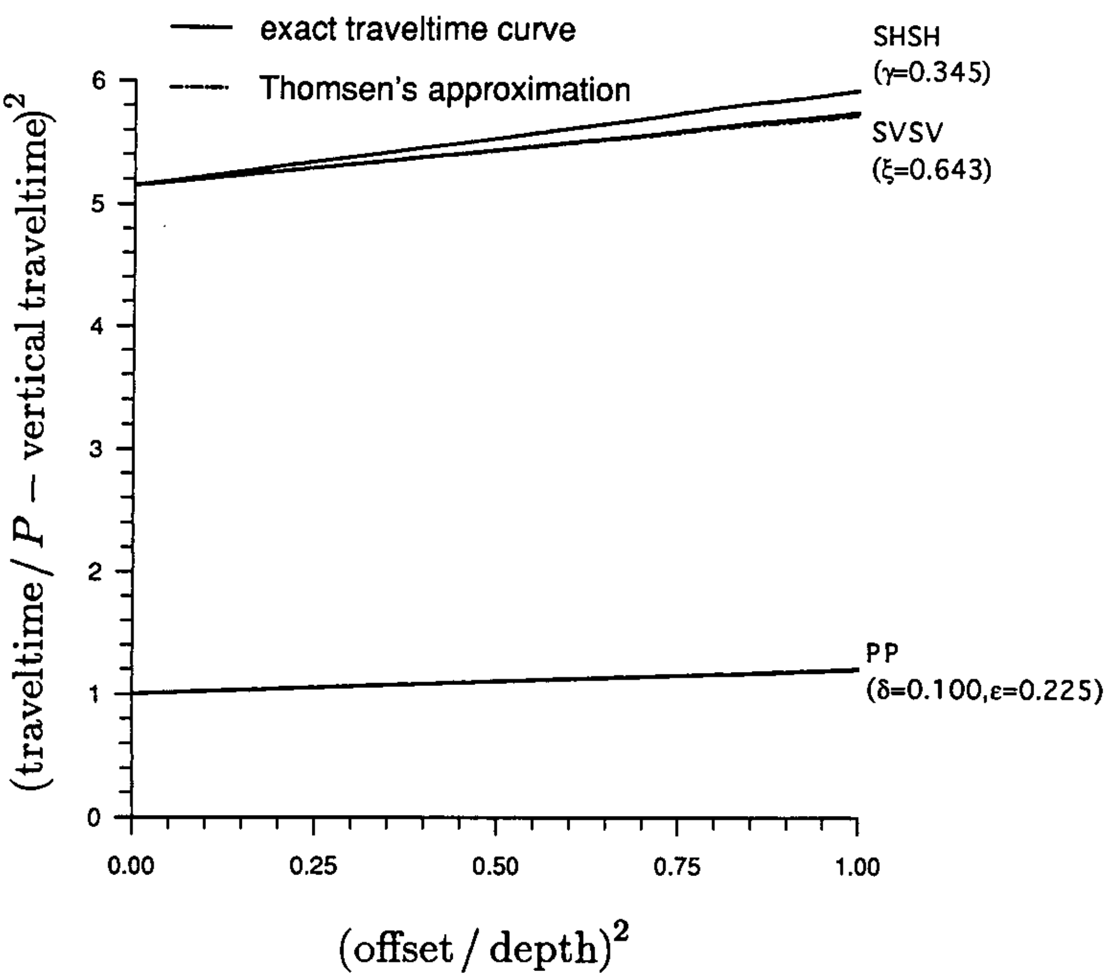

FIG. 6: Exact and approximate traveltime curves of Dog Creek shale. Due to no convexity of the *SVSV* traveltime curve indicated by a large positive anisotropy coefficient ξ, Thomsen's (1986) approximation of the NMO velocity is excellent in spite of a less perfect approximation of the wavefront.